

Quambalarine B, a Secondary Metabolite from *Quambalaria cyanescens* with Potential Anticancer Properties

Valéria Grobárová,^{†,‡} Karel Vališ,^{‡,§,‡} Pavel Talacko,^{‡,§} Barbora Pavlů,[†] Lucie Hernychová,^{†,‡} Jana Nováková,[‡] Eva Stodůlková,[‡] Miroslav Flieger,[‡] Petr Novák,^{‡,§} and Jan Černý^{*,†}

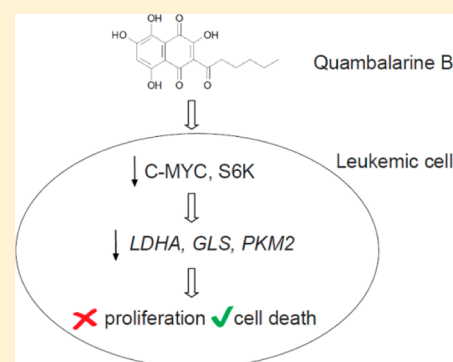
[†]Department of Cell Biology, Faculty of Science, Charles University, Viničná 7, 128 43 Prague 2, Czech Republic

[‡]Institute of Microbiology, v.v.i., The Czech Academy of Sciences, Vídeňská 1083, 142 20 Prague 4, Czech Republic

[§]Department of Biochemistry, Faculty of Science, Charles University, Hlavova 8, 128 43 Prague 2, Czech Republic

Supporting Information

ABSTRACT: Quambalarine B (QB) is a secondary metabolite produced by the basidiomycete *Quambalaria cyanescens* with potential anticancer activity. Here we report that QB at low micromolar concentration inhibits proliferation of several model leukemic cell lines (Jurkat, NALM6, and REH), whereas higher concentrations induce cell death. By contrast, the effect of QB on primary leukocytes (peripheral blood mononuclear cells) is significantly milder with lower toxicity and cytostatic activity. Moreover, QB inhibited expression of the C-MYC oncoprotein and mRNA expression of its target genes, *LDHA*, *PKM2*, and *GLS*. Finally, QB blocked the phosphorylation of P70S6K, a downstream effector kinase in mTOR signaling that regulates translation of C-MYC. This observation could explain the molecular mechanism behind the antiproliferative and cytotoxic effects of QB on leukemic cells. Altogether, our results establish QB as a promising molecule in anticancer treatment.



During the long-term optimization of chemical interactions in complex ecosystems, mixtures of synergistic biologically active chemicals evolved, with some of them being used as traditional medicines in many cultures. It is therefore not surprising that large numbers of potential drugs in clinical trials are either natural products or compounds derived from natural products. Given that, since the 1940s, 175 small molecules have been approved worldwide for the treatment of cancer, research on natural product-based therapeutics is obviously one of the most promising approaches.^{1,2}

Among the anticancer bioactive substances, there is an important structurally related group of plant- and fungi-derived quinones,^{3,4} namely, compounds belonging to the structurally diversified subgroup of quinones (i.e., the naphthoquinones).⁵ For example, the 1,2-naphthoquinone-based compound, β -lapachone, has been assessed for its antitumor activity against advanced solid tumors.⁶ Potent antileukemic activity of shikonin, a naphthoquinone isolated from *Lithospermum erythrorhizon* has recently been reported by Zhao et al. to inhibit C-MYC oncoprotein expression and activity in leukemic cells and to block AKT and ERK signaling pathways.⁷ Recently, we reported the isolation of a novel fungal secondary metabolite family of naphthoquinone derivatives from *Quambalaria cyanescens* (Basidiomycota: Microstromatales).⁸ One of these compounds showed striking cytostatic bioactivities in various cancer-derived cell lines. Its chemical structure was determined as 3-hexanoyl-2,5,7,8-tetrahydroxy-1,4-naphthoquinone (Quambalarine B; QB). The mode of action of QB in cancer cell lines is not known. One possible mechanism could be interference with

mitochondrial function (resulting in loss of the mitochondrial proton gradient)⁸ and subsequent compensatory alterations of cellular metabolism and cell cycle control described for other relevant naphthoquinones.⁹

Recent reports demonstrated inhibition of the PI3K-AKT-mTOR pathway as a new mechanism of shikonin action in leukemia cells.¹⁰ The activity of this pathway seems to be crucial for C-MYC expression and the transcription of C-MYC target genes.¹¹ The P70S6K kinase is one of the key molecules involved in the mTOR signaling pathway and regulates C-MYC translation.^{12,13} Recently, shikonin-mediated inhibition of C-MYC expression and a decrease in lactate production in leukemia cells was also demonstrated (Vališ et al., unpublished data). The structural similarities between QB and shikonin prompted us to test the effect of QB on C-MYC expression and P70S6K phosphorylation in selected leukemia cell lines.

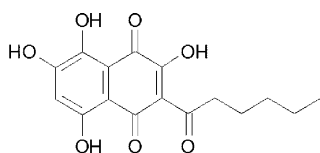
Because C-MYC represents a key driver oncogene of cancer cells, its inhibition represents one of the therapeutic approaches to leukemia treatment.¹⁴ C-MYC regulates genes involved in many cellular functions including metabolic processes. It controls gene expression directly, as in the case of *lactate dehydrogenase A* – *LDHA*, an essential glycolytic enzyme,¹⁵ or indirectly. Indirect targets involve glycolytic and glutaminolytic enzymes represented by glutaminase (*GLS*) and pyruvate kinase M2 (*PKM2*).^{16–18}

Received: May 17, 2016

The above-mentioned anticancer mechanisms target metabolism, which is profoundly altered in the majority of tumors. The existence of a metabolic switch in cancer cells was first postulated 70 years ago, claiming that most cancer cells obtain energy via glycolysis in the cytosol, instead of oxidation in mitochondria, even in the presence of oxygen.^{19,20} The importance of this phenomenon was highlighted by Hanahan and Weinberg who declared the reprogramming of energy metabolism a hallmark of cancer.²¹

In the present study, we report the antiproliferative and cytotoxic effects of QB on several human leukemic cell lines including Jurkat (T-lymphoma cells), NALM6 (pre-B-lymphoma cells), and REH (B cell precursor leukemia). We also studied the effect of QB on peripheral blood mononuclear cells (PBMC) to identify any differences between the QB effect on leukemic cell lines and on primary cell lines. Moreover, time- and concentration-dependent protein expression of C-MYC and activity of the P70S6K kinase involved in the mTOR signaling pathway in all leukemic cell lines was examined. Finally, gene expression of selected C-MYC target genes (*LDHA*, *GLS*, *PKM2*) involved in relevant cellular metabolic processes was studied.

Many secondary metabolites, presumably including the naphthoquinone quambalarine B produced by *Quambalaria cyanescens*, target general cellular processes conserved among different kingdoms of life (Fungi and Animalia). Quambalarine B belongs to the bioactive molecules, originally developed and structurally optimized via ecological constraints, which are potentially useful for the treatment of human diseases.⁸ The molecular mechanism of quambalarine B bioactivity (underlying the alteration of mitochondrial function in ecological competitors and human cell lines *in vitro*) fits to the mainstream of the research focused on development of novel effective anticancer treatments and strengthen its therapeutic potential.



Structure of quambalarine B (QB)

RESULTS AND DISCUSSION

Determination of Cytotoxicity EC_{50} for QB in Selected Leukemic Cell Lines. Bioactivity of QB and estimated effective concentrations (EC_{50}) for selected representative leukemic cell lines were studied using flow cytometry. For the detection of cells

with permeable cytoplasmic membranes (indicating loss of viability), cells were incubated with Hoechst 33258. The cell line most sensitive to QB treatment was Jurkat (derived from T-cell lymphoma) with cytotoxicity $EC_{50} = 7.41 \pm 0.33 \mu\text{mol/L}$ (Figure 1A). The NALM6 and REH cell lines were more resistant, with $EC_{50} = 16.68 \pm 0.95 \mu\text{mol/L}$ and $EC_{50} = 22.0 \pm 1.67 \mu\text{mol/L}$, respectively (Figure 1B,C).

Effect of QB on Proliferation of Selected Leukemic Cell Lines. Besides cytotoxicity, a cytostatic effect (usually observed at lower concentrations) is an important parameter for potential therapeutic use. Therefore, the effect of $2 \mu\text{mol/L}$ QB on cell proliferation was analyzed using a Bürker counting chamber or the Cell Proliferation Dye (CPD). Growth curves and the Population Doubling Levels (PDL) for each cell line in the presence or absence of QB were measured. It was found that proliferation was significantly blocked after 2–3 days of treatment for the Jurkat and REH cell lines and after 4–5 days for the NALM6 cell line (Figure 2A–C). This observation corresponded with significantly lower PDL after QB treatment for the Jurkat ($p = 0.0054$), NALM6 ($p = 0.012$), and REH cell lines ($p = 0.0034$), respectively. PDL for untreated/treated cells were: Jurkat-3.25/1.64, NALM6-3.44/1.75, REH-3.55/1.32 in a 6-day experiment (Figure 2D). To characterize the cytostatic effect in detail, a proliferation assay using FACS analysis was performed. Figure 2E shows a 5-day experiment overlay chart with individual cell divisions (% of live cells in the cell cultures and corresponding cell counts). Each day of the experiment, an identical volume of medium was removed from the cell culture, and therefore, we cannot compare the doubling times to the Bürker counting chamber experiment (see Experimental Section). To obtain comparable cell counts for each experimental day, samples were measured in the same volume. The data obtained by these two methods complement each other and indicate cell cycle arrest at concentrations around 1/4–1/11 of the respective EC_{50} . REH is obviously the most sensitive cell line, followed by Jurkat, and NALM6 as the most resistant. The same pattern was obtained using the well-established anticancer drug doxorubicin. The biggest difference between cytotoxicity (REH $EC_{50} = 22.0 \pm 1.67 \mu\text{mol/L}$) and a cytostatic effect mediated by QB in a low micromolar concentration was found in REH cells.

Effect of QB on Primary Peripheral Blood Mononuclear Cells (PBMC). For clinical use, there must be a significant EC_{50} difference between the primary cells and malignancies. To test the bioactivity of QB on primary cells, PBMC were analyzed, and striking differences between lymphocytes and monocytes were found (Figure 3A). Monocytes (CD14+ cells) were much more sensitive with an EC_{50} similar to leukemic cell lines ($EC_{50} = 15.10 \pm 0.69 \mu\text{mol/L}$). Representative dot plots (from biological

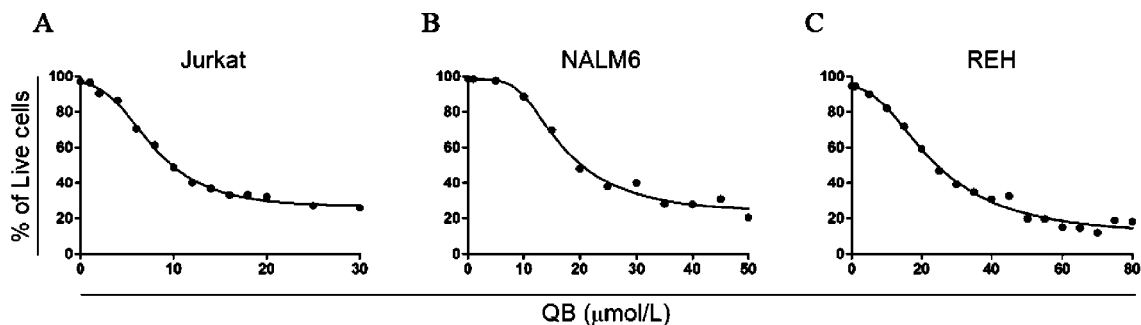


Figure 1. Determination of QB effective concentration (EC_{50}) in selected leukemic cell lines. (A–C) Percentages of live cells for the respective cell populations after 24 h of incubation with different concentrations of QB. Fractions of live cells were determined using Hoechst 33258 staining.

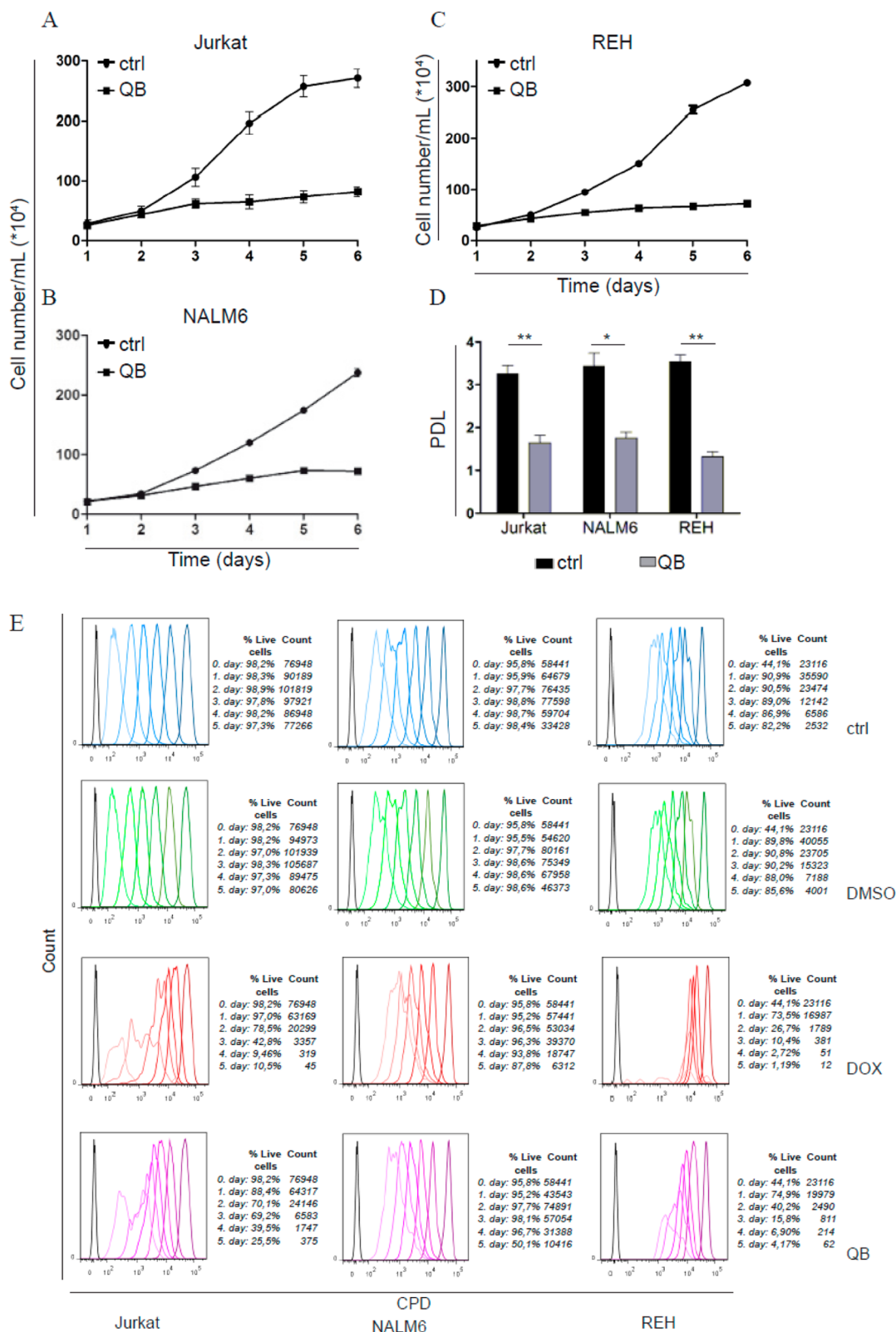


Figure 2. Effect of QB on cellular proliferation. (A–C) Growth curves of selected cell lines in the presence of 2 $\mu\text{mol/L}$ QB and in an untreated control (with DMSO). Cell numbers were determined each day during the indicated period using a Bürker counting chamber. (D) Effect of 2 $\mu\text{mol/L}$ QB on the Population Doubling Level (PDL). Results represent the average \pm standard deviation of values from three different experiments. Significant differences between QB treatments and the corresponding controls (DMSO) are marked by asterisks (* $p \leq 0.05$, ** $p \leq 0.01$). (E) FACS-based proliferation assay. Each cell line was treated with 2 $\mu\text{mol/L}$ QB for 5 days. Cells cultured only with RPMI (ctrl) or with DMSO (DMSO) served as negative controls. Doxorubicin (DOX) was used as a positive control in particular previously titrated concentrations for each cell line (Jurkat 10 ng/mL, REH 20 ng/mL, NALM6 5 ng/mL). Black histograms represent unlabeled cells, color grading represents individual cell divisions (cells labeled with CPD), with % of live cells in the cell cultures and corresponding cell counts, during a 5-day experiment.

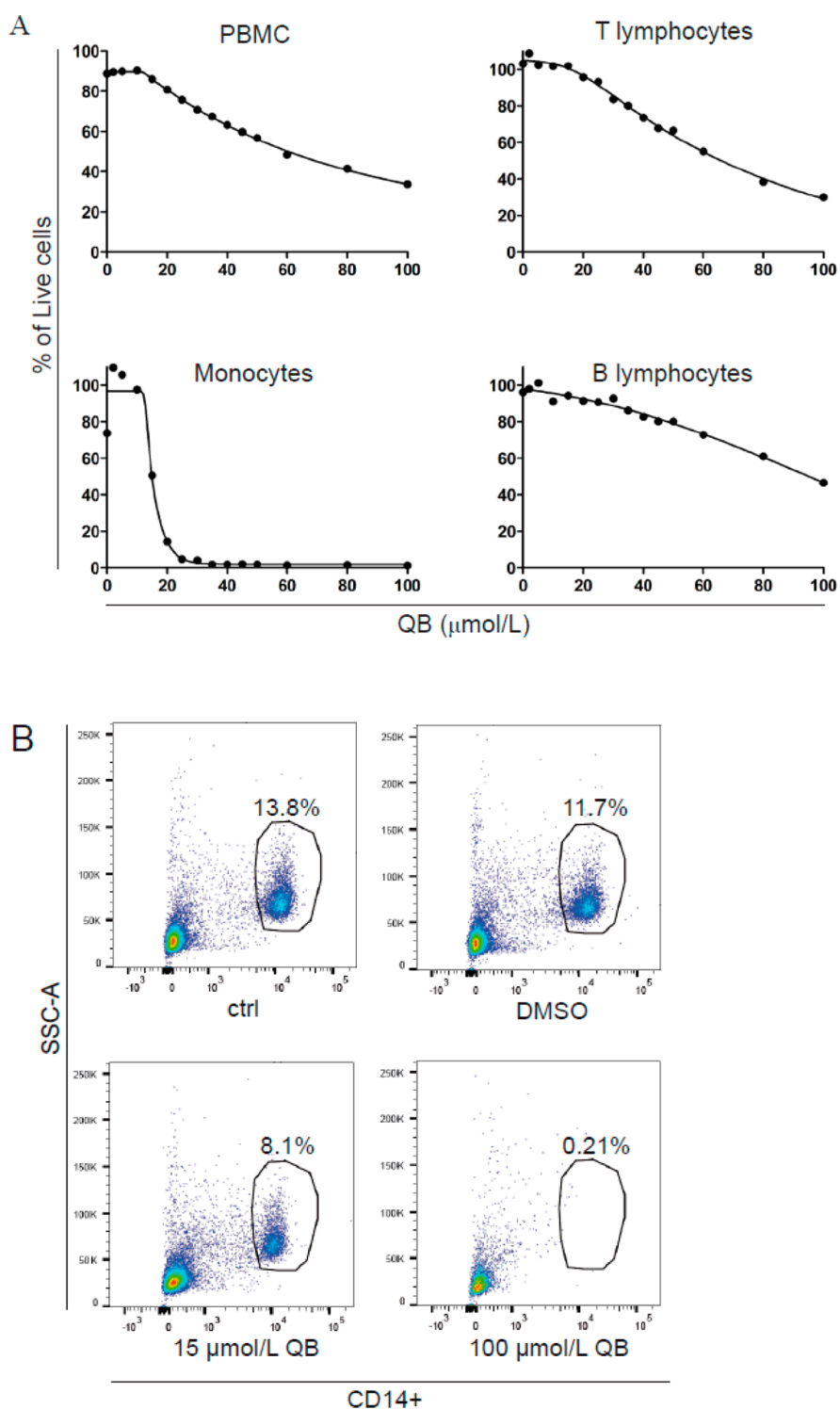


Figure 3. Determination of QB effective concentration (EC_{50}) in peripheral blood mononuclear cells (PBMC). (A) Percentages of live cells in the respective cell populations (PBMC, CD3+ T lymphocytes, CD14+ monocytes and CD20+ B lymphocytes) after 24 h of incubation with different concentrations of QB. Fractions of live cells were determined using Hoechst 33258 staining. (B) Representative dot plots indicating percentage decline of monocytes (CD14+) in PBMC population after 24 h of treatment with QB.

hexaplicate) on [Figure 3B](#) show the decline of monocyte population (CD14+) in PBMC after 24 h of treatment with QB. On the contrary, T lymphocytes (CD3+ cells) were much more resistant with an EC_{50} of $65.67 \pm 15.35 \mu\text{mol/L}$. Moreover, EC_{50} for B lymphocytes (CD20+ cells) within this QB concentration range was not possible to calculate. Overall, EC_{50} for PBMC was $56.09 \pm 3.07 \mu\text{mol/L}$.

During anticancer therapies, proliferation rates (and consequently activation and differentiation) of the immunocytes are often affected, potentially interfering with the normally highly enhanced anticancer immune response (activation of antigen presentation, induction of tumor-specific cytotoxic T lymphocytes, antibody responses against tumor-associated antigens, effector functions of cytotoxic NK cells).²² Therefore, we tested

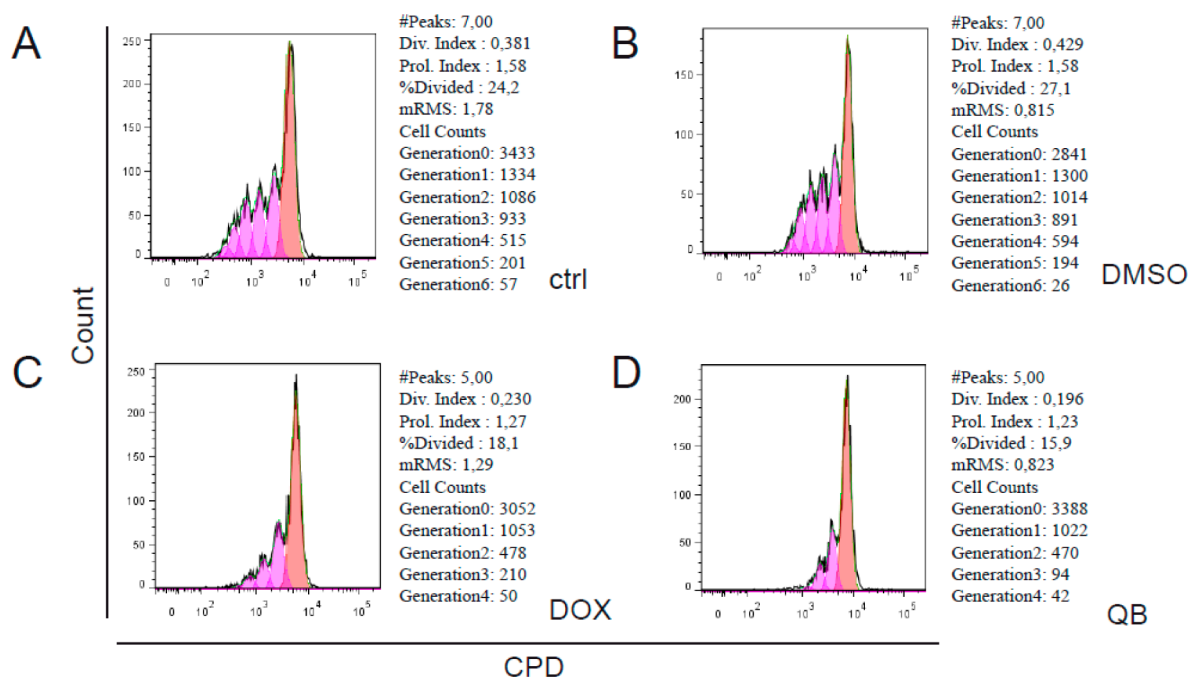


Figure 4. Effect of QB on T lymphocyte (CD3+) proliferation. PBMC were stained with the Cell Proliferation Dye (CPD) and stimulated with phytohemagglutinin (PHA) (5 $\mu\text{g}/\text{mL}$) and lipopolysaccharide (LPS) (1 $\mu\text{g}/\text{mL}$). After 18 h of stimulation, QB (2 $\mu\text{mol}/\text{L}$) was added and analyzed by FACS after 72 h of treatment. Doxorubicin (5 ng/mL DOX) was used as a positive control. Cells cultured in RPMI (ctrl) or in RPMI with DMSO (DMSO) were used as negative controls. The number of peaks corresponds to the number of cell divisions. The better the model fit, the lower the root mean square. (Div. Index: division index; Prol. Index: proliferation index; % Divided: % of dividing cells; RMS: the root mean square).

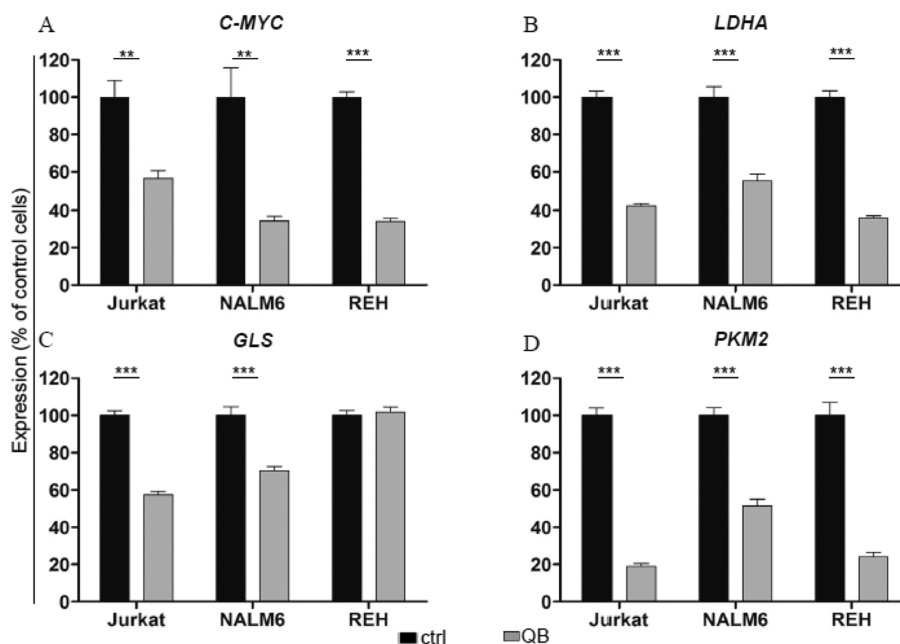


Figure 5. (A) Effect of QB on *C-MYC* mRNA levels. Cells were treated with concentrations of QB corresponding to EC_{50} for individual cell lines for 24 h. Relative expression of *C-MYC* mRNA was determined using RT-qPCR. Results represent the average \pm standard deviation of values from three different experiments. Significant differences between QB treatments and the corresponding controls (DMSO) are marked by asterisks (** $p \leq 0.01$, *** $p \leq 0.001$). (B–D) Effect of QB on expression of the *LDHA*, *GLS*, and *PKM2* genes (*C-MYC* target genes). Cells were treated with EC_{50} concentrations of QB for 24 h. Relative expression of selected targets of the *C-MYC* protein was determined using RT-qPCR. Results represent the average \pm standard deviation of values from three different experiments. Significant differences between QB treatments and the corresponding controls (DMSO) are marked by asterisks (** $p \leq 0.01$, *** $p \leq 0.001$).

the effect of QB (2 $\mu\text{mol}/\text{L}$) on the proliferation of T lymphocytes, which were the most resistant PBMC cell subpopulation. Lymphocytes were stimulated with phytohemagglutinin (PHA) (5 $\mu\text{g}/\text{mL}$) and lipopolysaccharide (LPS)

(1 $\mu\text{g}/\text{mL}$) for 18 h before QB (2 $\mu\text{mol}/\text{L}$) or doxorubicin treatment. Nonactivated CPD+ cells served as a reference to define the threshold for positive proliferation responses (as described in the [Experimental Section](#)). [Figure 4](#) shows the last

day of a 3-day experiment with the number of peaks representing the number of individual cell divisions. In negative controls (ctrl, DMSO), 7 peaks of CD3+ lymphocyte populations corresponding to 6 consecutive cell divisions with the proliferation index PI = 1.58 (Figure 4A,B) were observed. A 3-day incubation with QB or doxorubicin obviously decreased the cell division rate (number of peaks = 5) with PI = 1.23 and PI = 1.27, respectively (Figure 4C,D). Similar results were obtained comparing the division index and % of divided cells with a diluted proliferative fluorescent sensor CPD. The observed antiproliferative effect of QB is similar to the established anticancer drug doxorubicin at 5 ng/mL.

Effect of QB on the C-MYC Oncogene and C-MYC Target Genes. To understand the molecular mechanisms behind the bioactivity of QB, further research was focused on C-MYC, because it represents a key driver oncogene and influences uncontrolled proliferation. Individual cell lines were treated for 24 h with appropriate EC₅₀ concentrations of QB. Using RT-qPCR, significant decreases in C-MYC mRNA levels in all cell lines tested was found (Figure 5A).

Moreover, C-MYC links cellular metabolism to carcinogenesis.²³ Lower expression levels of LDHA and PKM2 in all tested cell lines were detected. Gene expression of GLS was significantly lower in the Jurkat and NALM6 cell lines. The only exception in the pattern of C-MYC target gene expression was observed in the REH cell line, where the GLS transcript was not changed, indicating cell-type-dependent variability in transcriptional control signaling and therefore variability in the response to QB treatment. Altogether, our transcriptional data support the hypothesis that C-MYC is directly involved in the molecular mechanism of QB impact on cellular metabolism (Figure 5B–D).

Effect of QB on C-MYC Oncoprotein Levels and mTOR Signaling. To complement the mRNA data, the effect of EC₅₀ concentrations of QB on C-MYC protein levels in a time-dependent manner using immunoblot was tested. Decreased C-MYC levels after 24 h of incubation with EC₅₀ concentrations of QB in all three leukemic cell lines were observed. In addition, the effect of QB on C-MYC levels in a concentration-dependent manner was tested. For individual cell lines, different QB concentrations in ranges from zero to the respective EC₅₀ were selected. Increasing concentration of QB resulted in a gradual decrease in C-MYC levels in all cell lines tested. One of the QB effects observed in the pilot study was an alteration of the mitochondrial network and a lack of the corresponding proton gradient.⁸ One possible link between the energy metabolism and proliferation control could be the P70S6K kinase, particularly its activation by phosphorylation. This protein is a downstream effector kinase in mTOR signaling and regulates translation of the C-MYC oncoprotein.²⁴ In Jurkat cells, QB at the EC₅₀ inhibits expression of unphosphorylated P70S6K protein, which is accompanied by the almost complete lack of phosphorylated P70S6K in a time-dependent manner, and this inhibition correlates with a decrease in C-MYC protein levels. Phosphorylation of P70S6K and levels of unphosphorylated P70S6K protein were also gradually inhibited after 24 h of treatment in Jurkat cells across all selected concentrations of QB (Figure 6A). In REH cells, P70S6K phosphorylation was gradually inhibited in a time- and concentration-dependent manner after 24 h of treatment with the EC₅₀ concentration of QB. EC₅₀ concentration of QB inhibited also levels of unphosphorylated P70S6K protein after 24 h of treatment. This time- and concentration-dependent effect of QB on P70S6K phosphorylation correlates

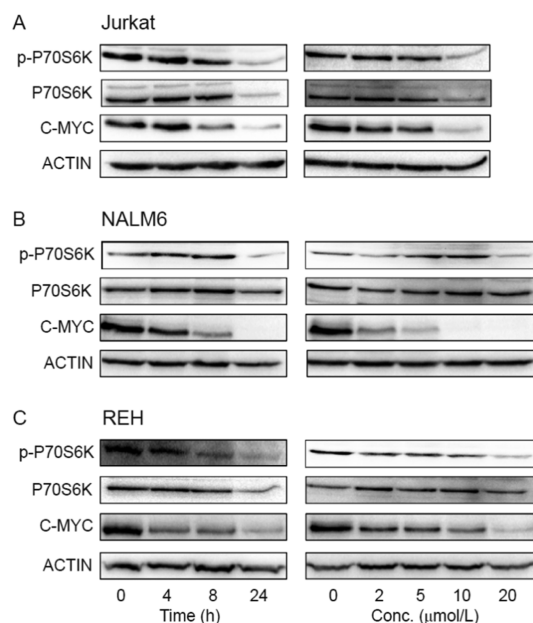


Figure 6. Effect of QB on C-MYC, P70S6K levels and phosphorylation of P70S6K kinase in Jurkat, NALM6, and REH cell lines. Cells were treated with EC₅₀ concentrations of QB for the indicated time periods or with specified concentrations of QB for 24 h. Levels of the C-MYC protein, P70S6K protein, and the active p-P70S6K kinase were detected using immunoblot.

with the effect on C-MYC protein levels (Figure 6C). In NALM6 cells, the phosphorylation of P70S6K slightly increased during early periods (as well as P70S6K per se) of the treatment and was strongly inhibited after 24 h of treatment with the EC₅₀ concentration of QB. A similar effect was observed also for the concentration-dependent treatment. QB has a minor effect on unphosphorylated P70S6K protein in NALM6 cells during all performed experiments. The effect of QB on C-MYC levels did not correlate with its effect on P70S6K phosphorylation; C-MYC protein levels gradually decreased in a time- and concentration-dependent manner in NALM6 cells (Figure 6B). These immunoblotting data show that the crosstalk between cellular metabolism and cellular proliferation mediated by the mTOR downstream effector kinase P70S6K and the C-MYC oncoprotein could be altered by the novel naphthoquinone QB. C-MYC inhibition by QB may constitute a novel approach to leukemia treatment.

When chemotherapy is used as anticancer treatment, its drawbacks are dose-limiting toxicity related to drug resistance²⁵ and severe side effects throughout the body.^{26,27} Therefore, for the discovery of new compounds with better specificity and fewer off-target effects is needed to improve therapy. Organisms involved in long-term competitive ecological interactions represent an excellent source of bioactive compounds, including those with anticancer properties. Many species of plants and fungi have been used for centuries in traditional medicines. Among these, the Chinese traditional medicines have a prominent place. Recent research confirmed bioactivity for several of these compounds, and relevant data published mostly in the Chinese literature were recently summarized by Wang et al., with a focus on natural products identification, their ability to overcome cancer, and cell drug resistance.²⁸

We previously reported that the biological activity of QB was selective at the cellular level toward mitochondria, which was undetectable using a mitochondrial proton gradient probe.⁸ The

QB structure is based on a naphthoquinone chromophore, like many other natural products and several synthetic drugs.⁵ Hence, we decided to use another complex naphthoquinone, doxorubicin (DOX), a chemotherapeutic well-established in medical practice, as a relevant experimental control for QB. The toxicity of doxorubicin during anticancer therapy is well-known.^{29–31} In addition to other effects, DOX induces apoptosis by an oxidative stress mechanism and loss of mitochondrial membrane potential,³² an effect similar to that we observed for QB.⁸

To obtain a similar cytotoxic effect for QB and DOX during a 5-day proliferation experiment (data not shown), DOX concentrations were titrated to nanomolar levels (significantly lower compared to QB). This concentration difference is not surprising taking into account the obviously different mechanisms of action of these two molecules. Doxorubicin intercalates into the DNA and causes histone eviction from transcriptionally active chromatin,^{33–35} interferes with replication by inhibiting topoisomerase II progression,^{36,37} and triggers DNA damage response, or epigenome and transcriptome deregulation.³⁴ In this case, when the targeted molecule is DNA itself, low concentrations of the bioactive compound could start a cascade of cytotoxic events. The mode of action of QB is different; it most probably interferes with metabolic processes in a stoichiometric manner, and therefore, the need for a higher effective concentration is reasonable.

The effective antiproliferative concentration of QB is within the concentration range of established anticancer drugs routinely used for treatment of patients. Namely, methotrexate, when used as part of a combination therapy (for acute lymphoblastic leukemia, non-Hodgkin lymphoma, or osteosarcoma), is administered at a high dose (e.g., to overcome the mechanisms of cellular resistance), peak methotrexate plasma concentration can reach C_{\max} values $>1000 \mu\text{M}$ in 96% of patients.^{38,39}

As a side effect of chemotherapy, the destruction of bone marrow structure is observed, affecting the production of new blood cells and therefore reducing white blood cell counts.^{40–42} Obviously, there is a need for new drugs with limited toxicity toward hematopoiesis. Our results showed that only monocytes are susceptible to QB, while lymphocytes were only moderately affected, and only by very high QB doses ($>65 \mu\text{mol/L}$). Taking into consideration that the circulating physiological half-life of monocytes has been shown to be approximately 71 h in humans,⁴³ 42 h in rats,⁴⁴ and 17.4 h in mice,⁴⁵ they can quickly recover from stem cells, if the bone marrow is not damaged.

Concerning the molecular mechanism of action of QB, the results obtained here are comparable to the study by Zhao et al., showing that shikonin induces the inhibition of C-MYC gene and protein expression in leukemic cell lines together with the ERK/JNK/MAPK and AKT pathways.⁷ Moreover, shikonin has a strong cytotoxic effect on some other cancer cell lines, including drug-resistant ones. Similar to our observation with QB,⁸ its mechanism of action involves direct targeting of mitochondria, inducing a breakdown of the membrane potential.⁹ A study by Wiench et al. showed an inhibitory effect of shikonin on the IGF1R-Akt-mTOR signaling cascade (axis),¹⁰ which corresponds with our WB data showing that the mTOR downstream effector kinase P70S6K could be affected by QB.

C-MYC represents a driver oncogene in several cancer cell lines, and its activity is tightly connected to the expression of key metabolic enzymes involved in glycolysis and glutaminolysis.²³ Increased expression of LDHA represents a hallmark of cancer metabolism and is indispensable for lactate production by cancer cells and Warburg phenotype establishment.⁴⁶ In our experi-

ments, significantly decreased expression of LDHA in all leukemic cell lines tested was found. Because LDHA represents a direct target of the C-MYC oncoprotein, our results suggest inhibition of C-MYC transcriptional activity by QB. PKM2 represents an indirect target of C-MYC amplified in cancer cells. The PKM2 isoform is a result of alternative splicing of the PKM pre-mRNA, which is orchestrated by C-MYC targets acting as splicing factors.¹⁸ The PKM2 isoform exists in the cytosol also as a dimer with catalytic activity significantly lower compared to the PKM1 or PKM2 tetramer. The decreased catalytic activity of the PKM2 isoform results in the accumulation of upstream glycolytic metabolites and inhibition of oxidative phosphorylation, protecting proliferative cells from oxidative stress.⁴⁷ A decrease in the PKM2 isoform-specific mRNA was detected in all cell lines tested, which corresponds with decreased C-MYC transcriptional activity. The last tested indirect target of C-MYC was GLS, an enzyme involved in glutamine metabolism. C-MYC inhibits the expression of a miRNA which inhibits translation of the GLS mRNA, resulting in increased expression of the GLS protein.¹⁶ As well as other C-MYC targets, expression of GLS significantly decreased in two out of three cell lines tested except for the REH cell line. These results imply that GLS expression in REH cells may be regulated by proteins other than C-MYC. A similar scenario can be considered also for the Jurkat and NALM6 cell lines due to the lower level of inhibition of GLS expression in comparison with LDHA and PKM2. Based on our observations, QB interferes with the regulation of cellular metabolism and exhibits anticancer activity. This effect is mediated at least partially by inhibition of the C-MYC oncoprotein expression.

Altogether, our results describe QB as a promising compound with prospective anticancer properties. QB blocks proliferation of the model leukemic cell lines at low micromolar concentrations. Primary cells of adaptive immunity, the T and B lymphocytes, are resistant to the QB-mediated cytotoxicity (with EC_{50} above $50 \mu\text{mol/L}$) but partially sensitive to the cytostatic effect at low micromolar concentrations. Monocytes are the cell type most sensitive to the cytotoxic effect, but being part of the innate immunity, they could easily recover from stem cells after *in vivo* QB treatment.⁴³ The effect of QB is obviously cell-type-dependent and probably reflects the type of cellular metabolism and proliferative or differentiation programs. A tempting interpretation of the QB selective bioactivity toward leukemic cell lines is its interference with the cancer cell metabolism switched to a glycolytic mode, where new specific targets appear. The actual antitumor potential of QB is currently being tested using *in vivo* models, because results from *in vitro* experiments can explain the molecular mechanisms behind bioactivity, but they can provide only limited insight into pharmacokinetics and interactions with real cancer cases in general. Taking into account the limitations of an *in vitro* approach, our data explain to some extent the molecular mechanism behind QB action, namely, its antiproliferative and cytotoxic effects on leukemic cells.

■ EXPERIMENTAL SECTION

General Experimental Procedures. Methodologies for the submerged cultivation of the strain *Quambalaria cyanescens*. The method for compound extraction, isolation, and structure determination was published earlier.⁸

Briefly, the stock culture of the monospore strain *Q. cyanescens* CCM 8372 was maintained on malt agar slants and cultivated on a Czapek-Dox liquid medium. Submerged cultivations were carried out in 250 mL Erlenmeyer flasks on a rotary shaker for 21

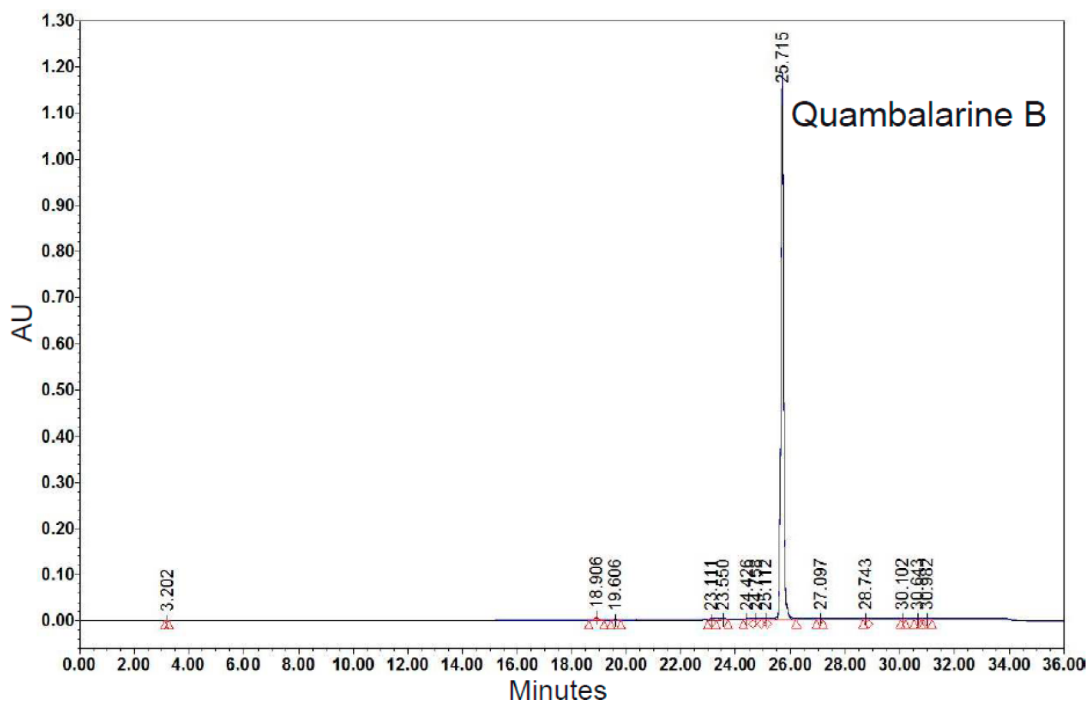


Figure 7. HPLC chromatogram of quambalarine B; determined purity 98.69%. Stock solution of quambalarine B (10 mL, 25 mM) was prepared by dilution of standard compound in DMSO. Aliquots (50 μ L) were kept frozen ($-20\text{ }^{\circ}\text{C}$) until use.

days at $24\text{ }^{\circ}\text{C}$ in the dark. The fermentation broth was centrifuged, filtered, and extracted with ethyl acetate containing 3% (V/V) of acetic acid. The crude extract evaporated to dryness was diluted in CH_2Cl_2 , subjected to gel chromatography on Sephadex LH-20 (GE Healthcare Bio-Science, Uppsala, Sweden), and eluted with a stepwise gradient of MeOH in CH_2Cl_2 . Fractions containing quambalarine B were collected and combined on the basis of their TLC profiles (toluene/ethyl acetate/TFA) and repeatedly crystallized from a solvent mixture of CH_2Cl_2 /MeOH. Structure elucidation was based on FTMS/MS and NMR spectrometry followed by X-ray crystallography. The purity of quambalarine B was tested by HPLC procedures described below.

HPLC Gemini 5 μ C18 column (250 mm \times 4.6 mm, Phenomenex, Torrance, CA, U.S.A.) with a guard column was used for the purity determination of quambalarine B. The mobile phase consisted of water (A) and methanol (B), both containing 1% TFA. Gradient elution started at 30% B (0 min), increasing linearly to 100% B within 20 min. Each analysis was followed by a column washing step (100% B, 10 min) and equilibration step (10 min), resulting in a total analysis time of 40 min. The flow rate was kept at 1.0 mL min^{-1} . UV detection was carried out at 295 and 270 nm.

A representative HPLC chromatogram of the standard compound (determined purity 98.69%) used throughout the study is presented in Figure 7. The HPLC system (Waters, Milford, MA, U.S.A.) consisted of a pump equipped with a 600E system controller, autosampler 717, and dual UV detector 2487. Data were processed with Empower 2 software. Water containing mobile phases was filtered through a $0.22\text{ }\mu\text{m}$ GS filter (Millipore, U.K.) and degassed in an ultrasonic bath for 10 min before use. The mobile phases were degassed continuously by sparking with helium at a rate of 40 mL min^{-1} . UV detection was carried out at 295 and 270 nm, respectively.

Cell Lines, Culture Conditions, and Reagents. The Jurkat, clone E6.1, (T lymphoblastoid cells) human cell line was

obtained from the ATCC collection (ATCC, Manassas, VA, U.S.A.). Both NALM6 (B cell precursor leukemia) and REH (B cell precursor leukemia) were kind gifts from Prof. J. Trka (Childhood Leukemia Investigation Prague, Czech Republic). All cell lines were cultured in the RPMI1640 medium with L-glutamine (Lonza Group, Ltd., Basel, Switzerland) supplemented with 10% fetal bovine serum (Gibco, Grand Island, NY, U.S.A.), 100 U/mL penicillin, and 100 $\mu\text{g/mL}$ streptomycin (PAA Laboratories, Pasching, Austria) in a humidified atmosphere at $37\text{ }^{\circ}\text{C}$ with 5% CO_2 .

Isolation of Peripheral Blood Mononuclear Cells (PBMC). PBMC were separated and isolated following the standard manufacturer's protocol using a Ficoll-Paque (GE Healthcare, Freiburg, Germany) density gradient. In brief, diluted blood samples (1:1 with PBS) were carefully layered on Ficoll-Paque and centrifuged at 400g for 30–40 min at $18\text{--}20\text{ }^{\circ}\text{C}$. The mononuclear cell layer at the interface was transferred to a new centrifugation tube for further PBMC isolation.

Determination of Effective Concentration (EC_{50}). EC_{50} values of QB for individual cell lines were estimated by seeding cells in flat-bottom 24-well plates at a density of 2×10^5 cells/mL and cultured in a final volume of 1 mL of RPMI1640. PBMC were seeded in U-bottom polypropylene 96-well plates at a density of 1×10^5 cells per well and cultured in a final volume of 400 μL of RPMI1640. Cells were treated with different concentrations of QB. Cells cultured in RPMI1640 and in RPMI1640 with DMSO only were used as negative controls. After 24 h of incubation, cells were harvested and washed with PBS with 0.02% gelatin and 0.01% sodium azide (Sigma-Aldrich, St. Louis, MO, U.S.A.). The phenotype of the respective PBMC populations was determined using the following monoclonal antibodies: anti-CD3-RPE, anti-CD14-biotin, anti-CD20-FITC (AbD Serotec, Kidlington, UK). The CD14 marker labeled with a biotinylated mAb in the first step was detected with a Streptavidin PE-Cy7 Conjugate (Thermo Fisher Scientific, Waltham, MA, U.S.A.). After staining with Hoechst 33258,

Table 1. Sequences of Primers Used in RT-qPCR Experiments

mRNA target	forward primer (5'-3')	reverse primer (5'-3')
<i>C-MYC</i>	TGGGATCTCTGCTCTCCTC	TGGGTTGTTGCTGATCTGTC
<i>LDHA</i>	CCCGACGTGCATTCCCGATT	TCTGGGGGGTCTGTTCTTCC
<i>GLS</i>	GGGTATGATGTGCTGGTCTC	CCACCTTCTCTTCGAGGATC
<i>PKM2</i>	TTCAAGTGCTGCAGTGGGGC	TGTCTGGGGATTCCGGGTCA
<i>RPLP0</i>	TCGACAATGGCAGCATCTAC	ATCCGTCTCCACAGACAAG

samples were measured with the FACS LSRII instrument (BD Biosciences, San Jose, CA, U.S.A.) and analyzed with the FlowJo 7.6.5 software (Tree Star, Ashland, OR, U.S.A.). EC_{50} was determined by five-parametric nonlinear regression using the GraphPad software v. 5.01 (San Diego, CA, U.S.A.). The Population Doubling Level (PDL) was calculated using the equation $PDL = \log(N_f/N_0)/\log 2$, where N_f = final number of cells and N_0 = initial number of cells.

Cell Proliferation. The effect of QB on proliferation of leukemic cell lines was monitored utilizing two methods. First, individual cell lines were seeded at a density of 2.5×10^5 cells/ml in control medium (with DMSO), and the medium was supplemented with QB at a concentration of $2 \mu\text{mol/L}$. Cell numbers were determined each day during the specified period using a Bürker counting chamber.

Second, the Cell Proliferation Dye (CPD) eFluor 670 (eBioscience, San Diego, CA, U.S.A.) was used to study proliferation. Cell lines were labeled with $5 \mu\text{mol/L}$ CPD following the manufacturer's protocol. Briefly, cells were washed several times with PBS to remove any serum and, while being vortexed, labeled with CPD and then incubated for 10 min at 37°C in the dark. Labeling was stopped by adding 5 volumes of cold complete medium (containing 10% serum) and incubating on ice for 5 min. Nonlabeled cells were used as a control for the following CPD cell toxicity quantification. Cell lines were seeded in flat-bottom 6-well plates at a density of 2×10^5 cells/mL in 2 mL of RPMI1640. Cells were treated with $2 \mu\text{mol/L}$ QB. Cells cultured in RPMI1640 and in RPMI1640 with DMSO were used as negative controls, cells treated with a particular concentration of doxorubicin optimized for each cell line (Jurkat 10 ng/mL – 17.25 nmol/L , REH 20 ng/mL – 34.5 nmol/L , NALM6 5 ng/mL – 8.625 nmol/L) served as positive controls. Doxorubicin concentrations were selected on the basis of the cytotoxicity effect of QB on individual cell lines during a 5-day experiment. Each day (after 24, 48, 72, 96, and 120 h of QB incubation) 1 mL of medium (out of 2 mL) containing the corresponding cell suspension was removed for measurement, and 1 mL of fresh medium was added with a particular concentration of QB, doxorubicin, and DMSO. The removed fraction of cells was harvested and washed with PBS with 0.02% gelatin and 0.01% sodium azide (Sigma–Aldrich). Live cells were determined using Hoechst 33258 staining. Samples were analyzed using the LSRII cytofluorometer (BD Biosciences) and individual cell divisions were analyzed with the FlowJo 7.6.5 software (Tree Star).

PBMC were stained with $1 \mu\text{mol/L}$ CPD according to the manufacturer's protocol and stimulated with phytohemagglutinin (PHA) ($5 \mu\text{g/mL}$) and lipopolysaccharide (LPS) ($1 \mu\text{g/mL}$) obtained from Sigma–Aldrich. Cells were seeded in U-bottom polypropylene 96-well plates at a density of 3×10^5 cells per well and cultured in a final volume of $300 \mu\text{L}$ of RPMI1640. As a control for cell toxicity, nonlabeled cells together with nonactivated cells were used. The unstimulated cells also served for assessing the CPD+ gate position. After 18 h of incubation with activators, $2 \mu\text{mol/L}$ QB was added. Doxorubicin (5 ng/mL

DOX) was used as a positive control. PBMC cultured in RPMI1640 and in RPMI1640 with DMSO were used as negative controls. For each time point (after 24, 48, 72 h of incubation with QB), the controls and treated cells were grown in individual plates. Cells were harvested at the indicated times, washed with PBS with 0.02% gelatin and 0.01% sodium azide (Sigma–Aldrich), and stained with an anti-CD3 monoclonal antibody (AbD Serotec) to determine the T lymphocyte population. As a secondary antibody, anti-IgG (H+L) Alexa Fluor 594 (Thermo Fisher Scientific) was used. Samples were measured by the LSRII cytofluorometer (BD Biosciences) and analyzed with the FlowJo v.7.6.5 software (Tree Star). The percentages of the cell populations were calculated from Hoechst 33258-negative singlets. To characterize the proliferation assay, the division index (DI), proliferation index (PI), and % of divided cells were used and calculated for CPD+CD3+ lymphocytes. PI represents the average number of divisions that all responding cells have undergone since stimulation/activation. DI compared to PI corresponds to the average number of divisions for all cells in the culture and % of divided cells defines what fraction of the original population divided at least once during the cultivation.⁴⁸

RNA Isolation, Reverse Transcription, and RT-qPCR Analysis. Jurkat, NALM6, and REH cells were seeded at a density of 7.5×10^5 cells/mL in 15 mL of the RPMI1640 medium and cultured overnight in 75 cm^2 cell culture flasks under standard cultivation conditions. Cells were treated with an appropriate EC_{50} concentration of QB dissolved in DMSO; an equal volume of DMSO was added to control cells.

Cultured cells were harvested (400g, 4 min) after 24 h of incubation, washed with PBS, and lysed in a cell lysis buffer (Aurum RNA Isolation Kit, Bio-Rad Laboratories, Hercules, CA, U.S.A.). Cell lysate was processed according to the manufacturer's protocol, including an on-column DNase treatment. The purified RNA was quantified and tested for the presence of contaminants with a NanoDrop spectrophotometer (Thermo Fisher Scientific). Reverse transcription of 700 ng of each purified RNA sample was performed using the M-MuLV *Taq* RT-PCR Kit (New England Biolabs, Ipswich, MA, U.S.A.). For individual RT-qPCR reaction mixtures, $2 \mu\text{L}$ of cDNA from the reverse transcription protocol was used. All reactions were run in triplicate using a CFX96 Real-Time PCR System (Bio-Rad) in final volumes of $25 \mu\text{L}$. Specific primers and the SsoFast EvaGreen Supermix (Bio-Rad) were used for amplification and fluorescent detection of PCR products. Relative expression of *C-MYC* was calculated using the Bio-Rad CFX manager.⁴⁹ The human ribosomal protein RPLP0 mRNA was used as a reference gene in all RT-qPCR experiments. The following primers were used in RT-qPCR for the quantification of *C-MYC*, *LDHA*, *GLS*, *PKM2*, and *RPLP0* mRNAs (Table 1).

SDS Electrophoresis and Immunoblotting. The same procedure as for RT-qPCR was used for cell preparation. Cells were washed with PBS supplemented with a Phosphatase Inhibitor Cocktail (Active Motif, La Hulpe, Belgium), lysed using the RIPA buffer (1% NP-40, 150 mM NaCl, 0.5% NaDOC, 0.1%

SDS and 50 mM Tris-HCl pH 8) supplemented with Complete Protease Inhibitor Cocktail Tablets (F. Hoffmann-La Roche Ltd., Basel, Switzerland), and incubated for 30 min on ice. The cell lysate was cleared via centrifugation (14 000g, 10 min, 4 °C). Bicinchoninic acid (BCA) assays were used to determine total protein concentration (BCA Protein Assay Kit, Thermo Fisher Scientific). SDS PAGE gels were loaded with 40 µg of protein per lane. A Protean III apparatus (Bio-Rad) with a constant voltage of 100 V was used to run the SDS PAGE protein samples. Separated proteins were blotted onto a nitrocellulose membrane (Pall Corporation, Port Washington, NY, U.S.A.) using a Trans-Blot SD Semi-Dry apparatus (Bio-Rad). Protein blots were blocked for 1 h in TBS supplemented with 5% milk (Bio-Rad) and 0.05% Tween-20 (Sigma-Aldrich). Membranes were then washed with TBS containing 0.05% Tween-20 and incubated with the respective primary and secondary antibodies according to manufacturer's protocols. The anti-C-MYC (Cell Signaling, Danvers, MA, U.S.A.), anti-Actin (Santa Cruz Biotechnology, Santa Cruz, CA, U.S.A.), anti-P70S6K (Cell Signaling, Danvers, MA, U.S.A.), and anti-p-P70S6K (Ser424, Santa Cruz Biotechnology) primary antibodies and goat antirabbit IgG-HRP and rabbit antigoat IgG-HRP (both from Santa Cruz Biotechnology) secondary antibodies were used for immunostaining.

■ STATISTICAL ANALYSIS

The statistical significance of differences between tested groups was calculated by Student's *t* test with a confidence interval of 95% using the GraphPad or QtiPlot software. The values of $p \leq 0.05$ (*), $p \leq 0.01$ (**), $p \leq 0.001$ (***) were considered to be statistically significant.

■ ASSOCIATED CONTENT

● Supporting Information

The Supporting Information is available free of charge on the ACS Publications website at DOI: [10.1021/acs.jnatprod.6b00362](https://doi.org/10.1021/acs.jnatprod.6b00362).

(PDF)

■ AUTHOR INFORMATION

Corresponding Author

*E-mail: jan.cerny@natur.cuni.cz. Tel.: +420-221-951-795. Fax: +420-221-951-761.

Author Contributions

[†]These authors contributed equally to this work (V.G. and K.V.).

Notes

The authors declare no competing financial interest.

■ ACKNOWLEDGMENTS

The Charles University (projects UNCE 204013/2012 and 204025/2012), Institutional Research Concept of the Institute of Microbiology (RVO61388971), European Regional Development Fund (BIOCEV CZ.1.05/1.1.00/02.0109), Czech Science Foundation (project nos. 13-16565S and 14-21095P), and Neuron Foundation.

■ REFERENCES

- (1) Newman, D. J.; Cragg, G. M. *J. Nat. Prod.* **2012**, *75*, 311–335.
- (2) Qurishi, Y.; Hamid, A.; Majeed, R.; Hussain, A.; Qazi, A. K.; Ahmed, M.; Zargar, M. A.; Singh, S. K.; Saxena, A. K. *Future Oncol.* **2011**, *7*, 1007–1021.
- (3) Lu, J. J.; Bao, J. L.; Wu, G. S.; Xu, W. S.; Huang, M. Q.; Chen, X. P.; Wang, Y. T. *Anti-Cancer Agents Med. Chem.* **2013**, *13*, 456–463.
- (4) Ferreira, I. C.; Vaz, J. A.; Vasconcelos, M. H.; Martins, A. *Anti-Cancer Agents Med. Chem.* **2010**, *10*, 424–436.
- (5) Wellington, K. W. *RSC Adv.* **2015**, *5*, 20309–20338.
- (6) Cragg, G. M.; Grothaus, P. G.; Newman, D. J. *Chem. Rev.* **2009**, *109*, 3012–3043.
- (7) Zhao, Q.; Assimopoulou, A. N.; Klauk, S. M.; Damianakos, H.; Chinou, I.; Kretschmer, N.; Rios, J. L.; Papageorgiou, V. P.; Bauer, R.; Efferth, T. *Oncotarget* **2015**, *6*, 38934–38951.
- (8) Stodulkova, E.; Cisarova, I.; Kolarik, M.; Chudickova, M.; Novak, P.; Man, P.; Kuzma, M.; Pavlu, B.; Cerny, J.; Flieger, M. *PLoS One* **2015**, *10*, e0118913.
- (9) Wiench, B.; Eichhorn, T.; Paulsen, M.; Efferth, T. *Evid. Based. Complement Alternat. Med.* **2012**, *2012*, ArticleNo. 726025.
- (10) Wiench, B.; Chen, Y. R.; Paulsen, M.; Hamm, R.; Schroder, S.; Yang, N. S.; Efferth, T. *Evid. Based. Complement Alternat. Med.* **2013**, *2013*, Article No. 818709.
- (11) Zhu, J.; Blenis, J.; Yuan, J. *Proc. Natl. Acad. Sci. U. S. A.* **2008**, *105*, 6584–6589.
- (12) Hofmann, J. W.; Zhao, X.; De Cecco, M.; Peterson, A. L.; Pagliaroli, L.; Manivannan, J.; Hubbard, G. B.; Ikeno, Y.; Zhang, Y.; Feng, B.; Li, X.; Serre, T.; Qi, W.; Van Remmen, H.; Miller, R. A.; Bath, K. G.; de Cabo, R.; Xu, H.; Neretti, N.; Sedivy, J. M. *Cell* **2015**, *160*, 477–488.
- (13) Faller, W. J.; Jackson, T. J.; Knight, J. R.; Ridgway, R. A.; Jamieson, T.; Karim, S. A.; Jones, C.; Radulescu, S.; Huels, D. J.; Myant, K. B.; Dudek, K. M.; Casey, H. A.; Scopelliti, A.; Cordero, J. B.; Vidal, M.; Pende, M.; Ryazanov, A. G.; Sonenberg, N.; Meyuhas, O.; Hall, M. N.; Bushell, M.; Willis, A. E.; Sansom, O. J. *Nature* **2015**, *517*, 497–500.
- (14) Landau, D. A.; Tausch, E.; Taylor-Weiner, A. N.; Stewart, C.; Reiter, J. G.; Bahlo, J.; Kluth, S.; Bozic, I.; Lawrence, M.; Bottcher, S.; Carter, S. L.; Cibulskis, K.; Mertens, D.; Sougnez, C. L.; Rosenberg, M.; Hess, J. M.; Edelman, J.; Kless, S.; Kneba, M.; Ritgen, M.; Fink, A.; Fischer, K.; Gabriel, S.; Lander, E. S.; Nowak, M. A.; Dohner, H.; Hallek, M.; Neuberg, D.; Getz, G.; Stilgenbauer, S.; Wu, C. J. *Nature* **2015**, *526*, 525–530.
- (15) Kim, J. W.; Zeller, K. I.; Wang, Y.; Jegga, A. G.; Aronow, B. J.; O'Donnell, K. A.; Dang, C. V. *Mol. Cell. Biol.* **2004**, *24*, 5923–5936.
- (16) Dang, C. V.; Le, A.; Gao, P. *Clin. Cancer Res.* **2009**, *15*, 6479–6483.
- (17) Wong, N.; De Mello, J.; Tang, D. *Int. J. Cell Biol.* **2013**, *2013*, Article No. 242513.
- (18) David, C. J.; Chen, M.; Assanah, M.; Canoll, P.; Manley, J. L. *Nature* **2010**, *463*, 364–368.
- (19) Warburg, O. *Science* **1956**, *123*, 309–314.
- (20) Dang, C. V.; Semenza, G. L. *Trends Biochem. Sci.* **1999**, *24*, 68–72.
- (21) Hanahan, D.; Weinberg, R. A. *Cell* **2011**, *144*, 646–674.
- (22) Bezu, L.; Gomes-de-Silva, L. C.; Dewitte, H.; Breckpot, K.; Fucikova, J.; Spisek, R.; Galluzzi, L.; Kepp, O.; Kroemer, G. *Front. Immunol.* **2015**, *6*, 187–197.
- (23) Stine, Z. E.; Walton, Z. E.; Altman, B. J.; Hsieh, A. L.; Dang, C. V. *Cancer Discovery* **2015**, *5*, 1024–1039.
- (24) Law, B. K.; Waltner-Law, M. E.; Entingh, A. J.; Chytil, A.; Aakre, M. E.; Norgaard, P.; Moses, H. L. *J. Biol. Chem.* **2000**, *275*, 38261–38267.
- (25) Paci, A.; Veal, G.; Bardin, C.; Leveque, D.; Widmer, N.; Beijnen, J.; Astier, A.; Chatelut, E. *Eur. J. Cancer* **2014**, *50*, 2010–2019.
- (26) Matsusaka, S.; Lenz, H. J. *Expert Opin. Drug Metab. Toxicol.* **2015**, *11*, 811–821.
- (27) Hodgson, D. C. *Clin. Adv. Hematol. Oncol.* **2015**, *13*, 103–112.
- (28) Wang, P.; Yang, H. L.; Yang, Y. J.; Wang, L.; Lee, S. C. *Evid. Based. Complement Alternat. Med.* **2015**, *2015*, Article No. 767136.
- (29) Buzdar, A. U.; Marcus, C.; Smith, T. L.; Blumenschein, G. R. *Cancer* **1985**, *55*, 2761–2765.
- (30) Muller, I.; Jenner, A.; Bruchelt, G.; Niethammer, D.; Halliwell, B. *Biochem. Biophys. Res. Commun.* **1997**, *230*, 254–257.
- (31) Wu, R.; Wang, H. L.; Yu, H. L.; Cui, X. H.; Xu, M. T.; Xu, X.; Gao, J. P. *Chem.-Biol. Interact.* **2016**, *244*, 149–158.

- (32) Mendivil-Perez, M.; Velez-Pardo, C.; Jimenez-Del-Rio, M. *Anticancer Drugs* **2015**, *26*, 583–598.
- (33) Fornari, F. A.; Randolph, J. K.; Yalowich, J. C.; Ritke, M. K.; Gewirtz, D. A. *Mol. Pharmacol.* **1994**, *45*, 649–656.
- (34) Pang, B.; Qiao, X.; Janssen, L.; Velds, A.; Groothuis, T.; Kerkhoven, R.; Nieuwland, M.; Ovaa, H.; Rottenberg, S.; van Tellingen, O.; Janssen, J.; Huijgens, P.; Zwart, W.; Neefjes, J. *Nat. Commun.* **2013**, *4*, 1908–1920.
- (35) Pang, B.; de Jong, J.; Qiao, X.; Wessels, L. F.; Neefjes, J. *Nat. Chem. Biol.* **2015**, *11*, 472–480.
- (36) Pommier, Y.; Leo, E.; Zhang, H.; Marchand, C. *Chem. Biol.* **2010**, *17*, 421–433.
- (37) Tacar, O.; Sriamornsak, P.; Dass, C. R. *J. Pharm. Pharmacol.* **2013**, *65*, 157–170.
- (38) Delepine, N.; Delepine, G.; Jasmin, C.; Desbois, J. C.; Cornille, H.; Mathe, G. *Biomed. Pharmacother.* **1988**, *42*, 257–262.
- (39) Crews, K. R.; Liu, T.; Rodriguez-Galindo, C.; Tan, M.; Meyer, W. H.; Panetta, J. C.; Link, M. P.; Daw, N. C. *Cancer* **2004**, *100*, 1724–1733.
- (40) Mariotta, S.; Aquilini, M.; Ricci, A.; Papale, M.; Pabani, R.; Sposato, B.; Mannino, F. *Eur. Rev. Med. Pharmacol. Sci.* **2002**, *6*, 67–73.
- (41) Liu, W.; Zhang, C. C.; Li, K. *Cancer Biol. Med.* **2013**, *10*, 92–98.
- (42) Yin, Q.; Chen, L.; Li, Q.; Mi, R.; Li, Y.; Wei, X.; Song, Y. *Cancer Cell Int.* **2014**, *14*, 85–95.
- (43) Whitelaw, D. M. *Cell Proliferation* **1972**, *5*, 311–317.
- (44) Volkman, A.; Collins, F. M. *J. Exp. Med.* **1974**, *139*, 264–277.
- (45) van Furth, R. *Curr. Top. Pathol.* **1989**, *79*, 125–150.
- (46) Le, A.; Cooper, C. R.; Gouw, A. M.; Dinavahi, R.; Maitra, A.; Deck, L. M.; Royer, R. E.; Vander Jagt, D. L.; Semenza, G. L.; Dang, C. V. *Proc. Natl. Acad. Sci. U. S. A.* **2010**, *107*, 2037–2042.
- (47) Wong, N.; Ojo, D.; Yan, J.; Tang, D. *Cancer Lett.* **2015**, *356*, 184–191.
- (48) Roederer, M. *Cytometry, Part A* **2011**, *79A*, 95–101.
- (49) Livak, K. J.; Schmittgen, T. D. *Methods* **2001**, *25*, 402–408.